Conformational Unfolding Studies of Three-Disulfide Mutants of Bovine Pancreatic Ribonuclease A and the Coupling of Proline Isomerization to Disulfide Redox Reactions†

Michio Iwaoka,‡ William J. Wedemeyer,§ and Harold A. Scheraga*

Baker Laboratory of Chemistry, Cornell University Ithaca, New York 14853-1301

Received October 30, 1998; Revised Manuscript Received December 29, 1998

ABSTRACT: The equilibrium stability and conformational unfolding kinetics of the [C40A, C95A] and [C65S, C72S] mutants of bovine pancreatic ribonuclease A (RNase A) have been studied. These mutants are analogues of two nativelike intermediates, des[40−95] and des[65−72], whose formation is rate-limiting for oxidative folding and reductive unfolding at 25 °C and pH 8.0. Upon addition of guanidine hydrochloride, both mutants exhibit a fast conformational unfolding phase when monitored by absorbance and fluorescence, as well as a slow phase detected only by fluorescence which corresponds to the isomerizations of Pro93 and Pro114. The amplitudes of the slow phase indicate that the two prolines, Pro93 and Pro114, are fully cis in the folded state of the mutants and furthermore that the 40−95 disulfide bond is not responsible for the quenching of Tyr92 fluorescence observed in the slow unfolding phase, contrary to an earlier proposal [Rehage, A., and Schmid, F. X. (1982) *Biochemistry 21,* 1499−1505]. The ratio of the kinetic unfolding $m^{\ddagger}$ value to the equilibrium *m* value indicates that the transition state for conformational unfolding in the mutants exposes little solvent-accessible area, as in the wild-type protein, indicating that the unfolding pathway is not dramatically altered by the reduction of the 40−95 or 65−72 disulfide bond. The stabilities of the folded mutants are compared to that of wild-type RNase A. These stabilities indicate that the reduction of des[40−95] to the 2S species is rate-limited by *global* conformational unfolding, whereas that of des[65−72] is rate-limited by *local* conformational unfolding. The isomerization of Pro93 may be rate-limiting for the reduction of the 40−95 disulfide bond in the native protein and in the des[65−72] intermediate.

Kinetic intermediates of protein folding are difficult to characterize structurally because the number of possible conformations is extremely large (*1*), and interconversion between conformations is rapid (*2*, *3*). However, structural insights can be obtained by coupling the conformation of the folding protein with changes in its covalent structure, particularly with the oxidation and reduction of disulfide bonds, since covalent intermediates are generally stable and thus easier to isolate and characterize than purely conformational intermediates.

Bovine pancreatic ribonuclease A (RNase A)[1] has long been a model protein for studying protein folding both conformationally and by oxidation of its sulfhydryl groups and reduction of its disulfide bonds (*4*−*6*). RNase A has four disulfide bonds (Cys26−Cys84, Cys58−Cys110, Cys40−Cys95, and Cys65−Cys72) of which the first two are completely buried and the latter two are mostly buried (Figure 1) (*7*, *8*). RNase A also has four prolines (Pro93, Pro114, Pro42, and Pro117) of which the first two are cis in the native conformation and the latter two are trans (Figure 1) (*7*, *8*). A method for tracking the isomerizations of specific prolines was developed recently (*9*), and it was shown that non-native isomers of Pro114, Pro117, and Pro93 cause increasing disruption of the conformational folding (*10*). A host of other methods, reviewed elsewhere (*4*−*6*), has been used to study the conformational folding of RNase A.

Recent research in our laboratory has focused on the oxidation of sulfhydryl groups and the reduction of disulfide bonds in RNase A at 25 °C and pH 8.0. Under these conditions, the oxidative folding of RNase A appears to proceed through several independent pathways, converging on *two* structurally ordered intermediates, des[65−72] and des[40−95] (*11*−*14*), whose formation is rate-limiting and

† This work was supported by research grant No. GM-24893 from the National Institute of General Medical Sciences of the National Institutes of Health.

* To whom correspondence should be addressed. Tel: (607) 255-4034. Fax: (607) 254-4700. E-mail: has5@cornell.edu.

‡ Visiting Scientist from the University of Tokyo.

§ NIH Trainee, 1993−1996.

[1] Abbreviations: RNase A, bovine pancreatic ribonuclease A; des[65−72], wild-type RNase A in which the 65−72 disulfide bond is reduced; des[40−95], wild-type RNase A in which the 40−95 disulfide bond is reduced; [C65S, C72S], the three-disulfide mutant of RNase A in which cysteines 65 and 72 have been replaced by serines; [C65A, C72A], the three-disulfide mutant of RNase A in which cysteines 65 and 72 have been replaced by alanines; [C40A, C95A], the three-disulfide mutant of RNase A in which cysteines 40 and 95 have been replaced by alanines; NMR, nuclear magnetic resonance; HPLC, high-performance liquid chromatography; MALDI−TOF, matrix-assisted laser desorption ionization−time-of-flight; DTT^{ox}, oxidized dithiothreitol; DTT^{red}, DL-dithiothreitol; AEMTS, 2-aminoethylmethanethiosulfonate; GdnHCl, guanidine hydrochloride; NTSB, disodium 2-nitro-5-thiosulfobenzoate; Tris, tris(hydroxymethyl)aminomethane; EDTA, ethylenediaminetetraacetic acid; BPTI, bovine pancreatic trypsin inhibitor.

10.1021/bi982593k CCC: $18.00
Published on Web 02/09/1999

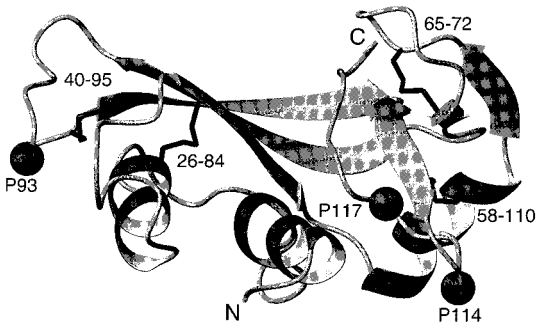

FIGURE 1: Ribbon diagram of RNase A taken from the structure of Wlodawer et al. (*7*). The four disulfide bonds are shown explicitly while the three essential prolines are represented by van der Waals spheres centered on their C^{α} atoms. The N and C termini are indicated by letters. This diagram was prepared with the program MOLMOL of Koradi et al. (*8*).

which are oxidized rapidly to the native form. The reductive unfolding of RNase A is likewise rate-limited by the same structured intermediates, des[65−72] and des[40−95], under a wide variety of conditions (*15*).

A kinetic analysis of the reductive unfolding of wild-type RNase A at pH 8.0 and 15−25 °C indicates that the native protein is reduced to the two structured intermediates, des-[65−72] and des[40−95], through two *independent, local* conformational unfolding events (*15*). The free-energy change in these local unfolding events is relatively large, roughly 5−6 kcal/mol (*15*), which is a significant fraction of the total free-energy change of unfolding, roughly 11 kcal/mol. The kinetics also suggest that only the 40−95 disulfide bond is reduced when the des[65−72] intermediate is reduced to the 2S species at pH 8.0 and 15 °C and, moreover, that this reduction occurs through the *same* local unfolding event which is rate-limiting for the reduction of the native protein to des[40−95] (*15*). However, the kinetics do not specify whether the des[65−72] intermediate is also reduced through local unfolding near the 40−95 disulfide bond at higher temperatures, for example, 25 °C, or whether the 65−72 disulfide bond is preferentially reduced in the des[40−95] intermediate under *any* conditions (*15*). The nature of these "independent local unfolding events" is undetermined and currently under investigation in our laboratory.

Proline isomerization is one candidate for these rate-limiting unfolding events. In particular, the reduction of the 40−95 and 65−72 disulfide bonds under strongly folding conditions (neutral pH and low denaturant concentration) might be accelerated strongly by the isomerizations of prolines (spatially) nearby in the native structure, specifically Pro93 for the 40−95 disulfide bond and Pro117 for the 65−72 disulfide bond (Figure 1). The isomerizations of these prolines from their native (cis and trans, respectively, for Pro93 and Pro117) to their non-native isomeric states qualify as independent local unfolding events, since the isomerization of any one proline does not unfold the native protein conformationally (*10*) and causes only a localized disruption of the structure, judging from the X-ray structures of the P93A and P114A mutants (*16*, *17*).

The equilibrium structures and redox kinetics of the two structured intermediates, des[40−95] and des[65−72], have been studied with site-directed mutant analogues, particularly [C40A, C95A], [C65A, C72A] and [C65S, C72S] (*13*, *18*, *19*). The folded structures of these mutants have been investigated by X-ray crystallography (*16*) and NMR spectroscopy (*19*, *20*) indicating that they both have a nativelike fold, albeit somewhat loosened, in agreement with the NMR structure of the des[65−72] intermediate blocked with AEMTS (*21*). The mutant and AEMTS-blocked structures constitute strong evidence that the *unblocked* des[65−72] and des[40−95] intermediates also have nativelike structures. These structural studies also suggest that the three essential prolines of RNase A (Pro93, Pro114, and Pro117) are in their native isomeric states in both the [C65S, C72S] and [C40A, C95A] mutants.

These mutant analogues resemble the two structured wild-type intermediates, des[65−72] and des[40−95], in their redox kinetics except that the disulfide rearrangement reactions which convert des[65−72] and des[40−95] into the unstructured 3S species in the wild-type protein (*15*) are blocked in the mutants. The elimination of the disulfide rearrangement reactions allows the redox reactions leading to and from the 2S species to be studied in isolation

$$\text{des}[65-72] + \text{DTT}^{\text{red}} \rightleftharpoons 2\text{S} + \text{DTT}^{\text{ox}} \qquad (1)$$

$$\text{des}[40-95] + \text{DTT}^{\text{red}} \rightleftharpoons 2\text{S} + \text{DTT}^{\text{ox}} \qquad (2)$$

The oxidative folding of the mutants has been investigated (*13*, *14*), but their reductive unfolding is just beginning to be studied (*22*).

In this paper, we measure the equilibrium stability and conformational unfolding kinetics of the mutants [C40A, C95A] and [C65S, C72S]. The equilibrium GdnHCl transitions are measured, from which the equilibrium *m* value and the standard free-energy difference, $\Delta G°$, between the folded and unfolded states are derived (*23*). By comparing the values of $\Delta G°$ for the mutants with the standard free energies of the rate-limiting unfolding steps in the reductions of the des-[65−72] and des[40−95] intermediates, we conclude that these intermediates are reduced to the 2S species though partial and global unfolding, respectively. Moreover, a further comparison of $\Delta G°$ for the mutants with the conformational destabilization for incorrect proline isomers (*9*) suggests that the isomerization of Pro93 from cis to trans may be the rate-limiting "local unfolding event" (*15*) which precedes the reduction of the native protein to des[40−95] and of the des-[65−72] intermediate to the 2S species. It is further proposed here that the isomerization of Pro117 is the local unfolding event which is rate-limiting for the reduction of the native protein to the des[65−72] species. Thus, proline isomerization may be coupled to critical redox reactions observed in RNase A.

It is also shown here that the fluorescence-monitored unfolding of the two mutants exhibits a fast and slow phase, as observed in wild-type RNase A (*24*). The slow fluorescence unfolding phase is independent of pH and GdnHCl concentration, and has an activation energy of 20 kcal/mol, which strongly suggests that the slow phase corresponds to the isomerizations of Pro93 and Pro114, as has been demonstrated for wild-type RNase A (*9*). The amplitudes of the slow unfolding fluorescence phase further imply that both prolines are fully cis in the folded mutants, consistent with the X-ray (*16*) and NMR data (*19*, *20*). The persistence of the slow unfolding phase in the [C40A, C95A] mutant

indicates that this phase does not arise from the fluorescence quenching of Tyr92 by the 40−95 disulfide bond, as previously proposed (*24*). The dependence of the fast phase unfolding time constant on GdnHCl concentration was also measured, and the kinetic unfolding $m^{\ddagger}$ value was obtained. The small ratio of $m^{\ddagger}$ to m indicates that the transition state of unfolding exposes little solvent-accessible surface area, as also observed for wild-type RNase A (*25*), indicating that the conformational unfolding pathway is not drastically altered by the reduction of the 40−95 and 65−72 disulfide bonds.

MATERIALS AND METHODS

Materials. Wild-type bovine pancreatic ribonuclease A type 1-A (Sigma) was purified by cation-exchange chromatography as described by Rothwarf and Scheraga (*26*). The three-disulfide mutants, [C40A, C95A] and [C65S, C72S], were expressed and purified by the procedures described by Laity et al. (*18*, *19*) and Shimotakahara et al. (*20*), respectively. The purity of the resulting mutant proteins was confirmed by cation-exchange HPLC, and their identities were confirmed by amino acid analysis and MALDI-TOF mass spectrometry. All other reagents were of the highest grade commercially available and used without further purification.

Determination of Extinction Coefficient. All of the absorbance measurements in this study were carried out with a modified Cary model 14 spectrophotometer (*27*). The molar extinction coefficients of the mutant proteins were determined by means of an NTSB assay for disulfides (*28*). By using these extinction coefficients at 275 nm in 100 mM acetic acid (8900 ± 200 and 8650 ± 100 M^{-1} cm^{-1} for [C65S, C72S] and [C40A, C95A], respectively), we determined the concentrations of the mutants. The concentration of wild-type RNase A was determined by using the extinction coefficient of 9600 M^{-1} cm^{-1} reported by Juminaga et al. (*10*).

Differences in extinction coefficients at 287 nm ($\Delta\epsilon_{287}$) between the folded and unfolded proteins were determined at room temperature. The folded protein was prepared by diluting the protein stock solution (8.6 mg/mL in 100 mM acetic acid) 21-fold with 100 mM Tris and 1 mM EDTA at pH 8.0, while the unfolded protein was prepared by diluting the stock solution 21-fold with 4.2 M GdnHCl, 100 mM Tris, and 1 mM EDTA at pH 8.0 so that the final concentration of GdnHCl was 4.0 M. The concentration of the protein in the stock solution was determined as described above. The concentration of GdnHCl was determined by measuring the refractive indices of the solutions at 25 °C (*29*) using a Bausch & Lomb refractometer.

Guanidine Hydrochloride Equilibrium Unfolding. The GdnHCl-unfolding transition curves were measured for wild-type RNase A (0.34 mg/mL), [C65S, C72S] (0.33 mg/mL), and [C40A, C95A] (0.36 mg/mL) in 100 mM Tris buffer at 25 °C and pH 8.0 by using the change in absorbance at 287 nm as a function of GdnHCl concentration. The temperature of the sample cell holder was maintained using a Neslab RTE-100 circulating bath interfaced to a SUN IPC computer. The temperature was measured to within 0.1 °C by using a calibrated thermistor placed in a buffer-containing cell located in a second compartment of the cell holder. Solutions were allowed to equilibrate at 25 °C for 1 h prior to measurement. The transitions were analyzed by the method described by Santoro and Bolen (*30*).

Optically Detected Kinetic Unfolding. A Hi-Tech Scientific PQ/SF-53 stopped-flow instrument was used to measure absorbance and fluorescence to follow the unfolding kinetics. The instrument has been described previously (*31*). The flow cell had a path length of 10 mm and a width of 2 mm. The measurements were carried out at 15 and 25 °C. For absorbance measurements, a deuterium lamp (Hellma) was used as a light source, and the monochromator for the incident light was set at 287 nm. For fluorescence measurements, a xenon arc lamp (Ushio, Japan) was used; the excitation wavelength was set at 268 nm, and a band-pass filter (280−400 nm) was used for emission. Data were collected every 0.5 ms for the first second and every 40 ms thereafter for up to 10 min.

For the single-jump unfolding experiments of wild-type RNase A or [C65S, C72S] at pH 2.0, the protein solution in 50 mM sodium acetate at pH 5.0 containing 0.6 M GdnHCl was mixed (1:10) with the unfolding buffer (4.34 M GdnHCl, 50 mM glycine at pH 1.77) so that the resulting solution contained 4.0 M GdnHCl at pH 2.0. For the unfolding experiments of [C65S, C72S] at pH 8.0, the protein solution in 100 mM Tris and 1 mM EDTA at pH 8.0 containing 0.6 M GdnHCl (or alternatively, free from GdnHCl) was mixed (1:10) with the unfolding buffer (100 mM Tris, 1 mM EDTA at pH 8.0) containing an appropriate amount of GdnHCl. The final concentration of GdnHCl was varied from 2.15 to 4.20 M in order to investigate the GdnHCl dependence of the unfolding time constants at 25 °C and pH 8.0. However, for unfolding of [C40A, C95A] at 25 °C and pH 8.0, the initial concentration of GdnHCl was always 0, and the final concentration was varied from 1.50 to 4.20 M. Final protein concentrations were approximately 0.3 mg/mL for all measurements. The fluorescence of the unfolded species was assigned the value of 100, and that of the folded species was assigned the value of 0. The data obtained from all stopped-flow measurements were fit to a sum of exponentials plus a constant baseline with the program PLOT from New Unit (Ithaca, NY), using a Levenberg−Marquardt algorithm (*32*) for nonlinear least-squares fitting. All errors are listed as standard deviations.

RESULTS

Differences in Extinction Coefficients ($\Delta\epsilon_{287}$). Differences in molar extinction coefficients at 287 nm ($\Delta\epsilon_{287}$) between the folded and unfolded proteins were determined in 100 mM Tris buffer at room temperature and pH 8.0; the results are shown in Table 1. The value of $\Delta\epsilon_{287}$ obtained for [C65S, C72S] (2900 M^{-1} cm^{-1}) was similar to that for the wild-type protein (3100 M^{-1} cm^{-1}), whereas that for [C40A, C95A] (2200 M^{-1} cm^{-1}) was significantly smaller. A recent disulfide-intact unfolding/refolding study of Tyr-to-Phe mutants of RNase A concluded that Tyr25, Tyr92, and Tyr97 are responsible for at least 90% of $\Delta\epsilon_{287}$ of RNase A (*10*). Since Tyr92 and Tyr97 are located close to the Cys40−Cys95 disulfide bond in the wild-type protein (Figure 1), the smaller value of $\Delta\epsilon_{287}$ obtained for [C40A, C95A] is probably due to a disruption of the native fold around Tyr92 or Tyr97. Tyr92 is much more likely than Tyr97, judging

Table 1: Summary of the Equilibrium Properties of Wild-Type RNase A and the Three-Disulfide Mutants in 100 mM Tris at 25 °C and pH 8.0

	$\Delta\epsilon_{287}$[a] (cm^{-1} M^{-1})	$\Delta G°(H_2O)$[b] (kcal mol^{-1})	m[b] (kcal mol^{-1} M^{-1})	$[GdnHCl]_{1/2}$[b] (M)
wild type	3100 ± 300	11.3 ± 0.7	3.8 ± 0.2	3.0 ± 0.2
[C65S, C72S]	2900 ± 200	5.0 ± 0.5	3.8 ± 0.4	1.3 ± 0.1
[C40A, C95A]	2200 ± 200	3.0 ± 0.2	3.9 ± 0.2	0.77 ± 0.05

[a] Differences in molar extinction coefficients at 287 nm at room temperature between the folded and unfolded proteins. The folded condition was 0 M GdnHCl, and the unfolded condition was 4.0 M GdnHCl. Errors are given as standard deviations. [b] The parameters were obtained by the method of Santoro and Bolen (*30*). $\Delta G°(H_2O)$ represents the estimated standard free-energy difference (unfolded minus folded) in water between the folded and unfolded protein. m represents the first derivative of the free-energy difference with respect to the concentration of GdnHCl. $[GdnHCl]_{1/2}$ represents the concentration of GdnHCl at the midpoint of the transition curves. Errors are given as standard deviations.

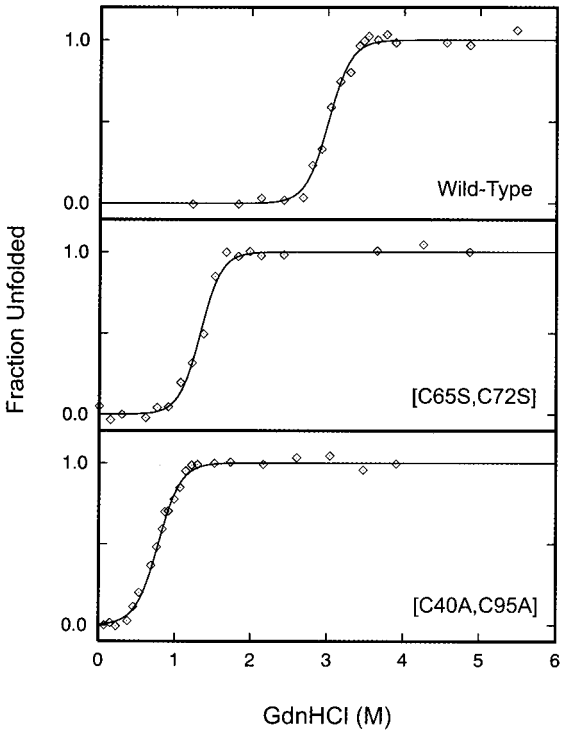

FIGURE 2: GdnHCl transition curves of wild-type RNase A and the three-disulfide mutants [C65S, C72S] and [C40A, C95A] at 25 °C and pH 8.0 in 100 mM Tris buffer, as followed by absorbance at 287 nm. The solid line represents the fit obtained by the method of Santoro and Bolen (*30*); the fitted parameters are given in Table 1.

from the X-ray structures of this mutant (*16*) and the corresponding NMR data (*19*). The value of $\Delta\epsilon_{287}$ obtained for the wild-type protein at pH 8.0 in the present study is roughly 350 M^{-1} cm^{-1} larger than that reported at lower pH (2749 M^{-1} cm^{-1} (*10*)); the difference is small, however, and may simply reflect more complete burial of Tyr92 at pH 8.0 than at pH 5.0 (*10*, *33*).

GdnHCl Transitions. The GdnHCl transition curves obtained by UV absorbance measurements at 287 nm in 100 mM Tris buffer at 25 °C and pH 8.0 are shown in Figure 2. The data were analyzed by assuming a two-state unfolding transition; the resulting unfolding free energies in water [$\Delta G°(H_2O)$], m values, and transition midpoints ($[GdnHCl]_{1/2}$) are given in Table 1. The value of $\Delta G°(H_2O)$ obtained for [C65S, C72S] (5.0 kcal/mol) is less than one-half of the wild-type value (11.3 kcal/mol), while that obtained for [C40A, C95A] (3.0 kcal/mol) is less than one-third of the wild-type value. Thus, the reduction of these disulfide bonds has decreased the conformational stability of the mutants significantly with respect to wild-type RNase A. On the other hand, similar m values were obtained for the mutant and wild-type proteins, indicating that similar amounts of surface area become exposed upon unfolding, consistent with the X-ray (*16*) and NMR (*19*, *20*) data. It should be noted that the transition region for [C40A, C95A] begins close to 0 M GdnHCl at 25 °C and pH 8.0.

Stopped-Flow Unfolding. Kinetic unfolding experiments of the three-disulfide mutants of RNase A were carried out under various conditions using a stopped-flow instrument. Figures 3 and 4 show representative stopped-flow traces obtained for [C65S, C72S] by absorbance and fluorescence measurements, respectively, in 4.2 M GdnHCl at 25 °C and pH 8.0. When the unfolding process was monitored by absorbance at 287 nm, only a fast phase was observed (Figure 3), whereas two phases (a fast and a slow phase) were clearly observed when the unfolding was monitored by fluorescence (Figure 4). The data were fit to a sum of exponentials plus a constant baseline, and the resulting time constants (τ_f and τ_s) and amplitudes (α_f and α_s) under various unfolding conditions are given in Table 2.

The fast unfolding phase and the slow unfolding phase can be reasonably assigned, respectively, to a purely conformational unfolding which exposes the buried tyrosines to solvent and to the cis−trans isomerization of X-Pro peptide bonds, for the following reasons. First, under identical unfolding conditions, two unfolding phases have also been observed for wild-type RNase A (Table 2), which have been definitively established as conformational unfolding and proline isomerization (*9*). The relative fluorescence amplitudes of the fast phase (α_f) and the slow phase (α_s) observed for [C65S, C72S] were similar to those observed for wild-type RNase A under identical conditions (Table 2B), and the slow unfolding time constant observed for [C65S, C72S] (τ_s = 64 s) was essentially identical to that for wild-type RNase A (τ_s = 67 s). Second, the activation energy for the slow unfolding phase of [C65S, C72S] is 20 kcal/mol (lines 3 and 4 of Table 2), in agreement with the known activation energy of proline isomerization (*34*) as well as the measured activation energies of proline isomerization in wild-type RNase A (*9*). Third, the time constant of the slow fluorescence unfolding phase did not depend on pH (Table 2) or upon guanidine concentration (Figure 5), consistent with proline isomerization (*9*), while that of the fast fluorescence unfolding phase did, consistent with conformational unfolding (*9*). Last, the time constant of the fast phase determined by absorbance measurements (τ_f = 17 ms) was nearly identical to that determined by fluorescence measurements (τ_f = 15 ms), showing that both methods monitor the same unfolding process; it is known that the absorbance changes monitor the exposure of buried tyrosines to the solvent and, thus, conformational unfolding (*9*).

The fast unfolding time constants measured for [C65S, C72S] (τ_f = 17 and 15 ms) were smaller than those for the wild-type protein (τ_f = 52 and 54 ms), indicating that the folded structure of the three-disulfide mutants can be broken down more easily by the denaturant, consistent with the lower

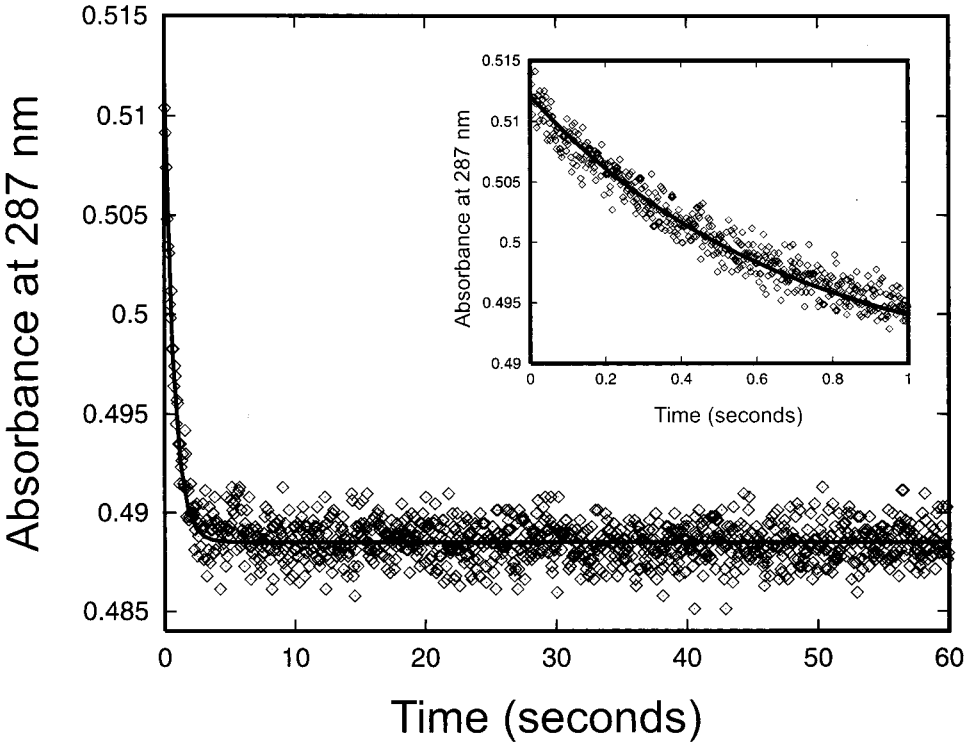

FIGURE 3: Representative data set showing the change in absorbance at 287 nm upon unfolding of the [C65S, C72S] mutant from 0.6 to 4.2 M GdnHCl at 25 °C and pH 8.0. Only a fast unfolding phase is observed by absorbance.

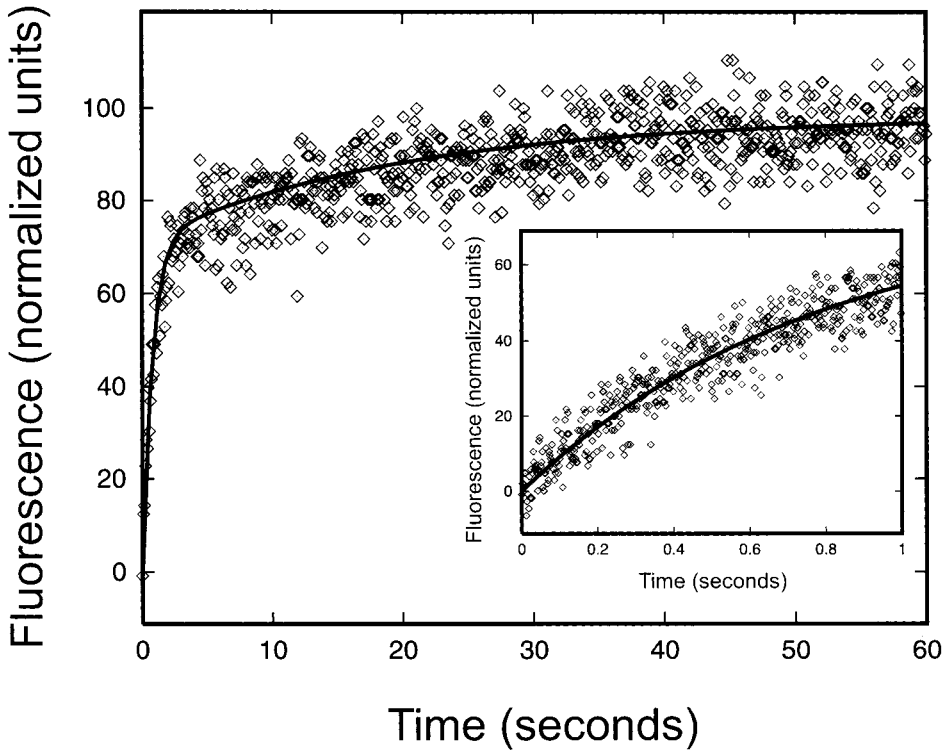

FIGURE 4: Representative data set showing the change in fluorescence upon unfolding of the [C65S, C72S] mutant from 0.6 to 4.2 M GdnHCl at 25 °C and pH 8.0. A fast phase ($\tau_f = 0.77$ s) and a slow phase ($\tau_s = 20$ s) were observed. Excitation was at 268 nm and the emission was detected using a band-pass filter (280−400 nm). The data are shown on a normalized scale.

conformational stabilities of the mutants relative to the wild-type protein (Table 1). The fast unfolding time constants exhibited a strong dependence on pH, increasing approximately 300-fold as the pH is increased from 2.0 to 8.0 (Table 2). Such dramatic increases have been observed before in the Y92W mutant of RNase A (*35*). This pH sensitivity is consistent with the pH dependence of the stability of RNase A (*36*, *37*) which has been hypothesized to derive from the protonation of the terminal carboxylate group (*38*), which is hydrogen-bonded to the backbone amide hydrogen of His105 in wild-type RNase A and in the [C65S, C72S] mutant (*20*). However, more careful studies are warranted to explain this pH sensitivity. The fast unfolding time constants also exhibited a strong dependence on temperature;

Table 2: Parameters Fitting the Single-Jump Unfolding[a] of Wild-Type RNase A and the Three-Disulfide Mutants under Various Conditions

protein	temperature (°C)	pH[b]	GdnHCl (M)[c]	fast phase, τ_f (ms) absorption[d]	fast phase, τ_f (ms) fluorescence[e]	slow phase, τ_s (s) fluorescence[e]
			Time Constants			
wild type	15	2.0	0.6 → 4.0	52 ± 3	54 ± 3	67 ± 3
[C65S, C72S]	15	2.0	0.6 → 4.0	17 ± 2	15 ± 2	64 ± 4
	15	8.0	0.6 → 4.2	5100 ± 200	5400 ± 200	63 ± 8
	25	8.0	0.6 → 4.2	690 ± 20	770 ± 40	20 ± 2
	25	8.0	0.0 → 4.2		760 ± 50	21 ± 2
[C40A, C95A]	25	8.0	0.0 → 4.2	52 ± 3	54 ± 9	18 ± 2
			Amplitudes			
wild type	15	2.0	0.6 → 4.0	0.028 ± 0.003	69 ± 3	31 ± 3
[C65S, C72S]	15	2.0	0.6 → 4.0	0.020 ± 0.002	71 ± 2	29 ± 2
	15	8.0	0.6 → 4.2	0.026 ± 0.001	75 ± 1	25 ± 1
	25	8.0	0.6 → 4.2	0.024 ± 0.001	72 ± 2	28 ± 2
	25	8.0	0.0 → 4.2		72 ± 4	28 ± 4
[C40A, C95A]	25	8.0	0.0 → 4.2	0.033 ± 0.002	66 ± 3	34 ± 3

[a] The single-jump unfolding was carried out under the conditions indicated in the Table. The final protein concentrations in all absorption and fluorescence measurements were approximately 0.3 mg/mL. [b] The final pH of the mixed solution. [c] The initial and final concentrations of GdnHCl. [d] The unfolding was monitored by absorption at 287 nm. The amplitudes are given in arbitrary units. Errors are given as standard deviations. [e] The unfolding was monitored by fluorescence. The excitation wavelength was 268 nm. For emission, a band-pass filter (280−400 nm) was used. The amplitudes (fluorescence increases) are in normalized units, where the fluorescence of the unfolded species was set to the value of 100 and that of the folded species was set to the value of 0. Errors are given as standard deviations.

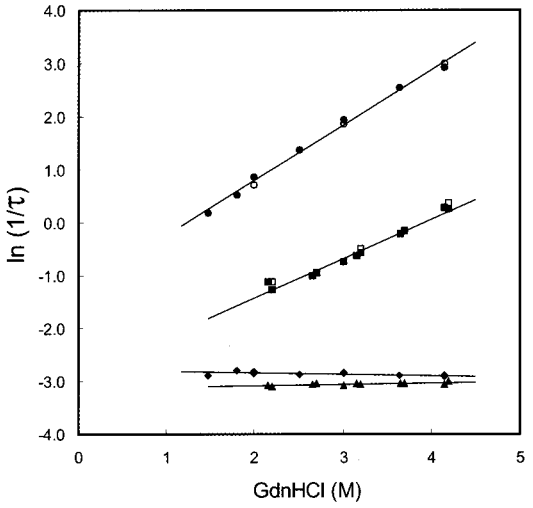

FIGURE 5: GdnHCl dependence of the time constants for unfolding of the [C65S, C72S] and [C40A, C95A] mutants at 25 °C and pH 8.0. The empty and filled squares represent the fast unfolding time constants of [C65S, C72S] as determined by absorbance and fluorescence measurements, respectively. The filled triangles represent the slow unfolding time constants of [C65S, C72S] as determined by fluorescence measurements. The empty and filled circles represent the fast unfolding time constants of [C40A, C95A] as determined by absorbance and fluorescence measurements. The filled diamonds represent the slow unfolding time constants of [C40A, C95A] as determined from fluorescence measurements.

the time constants decreased roughly 7-fold as the temperature was increased from 15 to 25 °C (Table 2).

The initial GdnHCl concentration does not seem to influence the unfolding. The [C65S, C72S] mutant was unfolded from initial GdnHCl concentrations ranging from 0.0 to 0.6 M, and neither the time constants nor the amplitudes of the fast and slow unfolding were affected. Presumably, the folded structures of [C65S, C72S] at 0.0 and 0.6 M GdnHCl are nearly identical, as expected from the GdnHCl transition curve of [C65S, C72S] (Figure 2). However, the transition region of the [C40A, C95A] mutant begins close to 0 M GdnHCl (Figure 2), and thus, this mutant was always unfolded from 0 M GdnHCl (Table 2).

The unfolding kinetics of both mutants were studied at pH 8.0 and 25 °C as a function of the final GdnHCl concentration (Figure 5). As noted above, the slow fluorescence unfolding phase was independent of guanidine concentration, consistent with its assignment as proline isomerization. On the other hand, the fast unfolding phases did depend on the final GdnHCl concentration and were well fit by the equation

$$\ln(1/\tau_f) = \ln(1/\tau_0) + m^{\ddagger}\frac{[\text{GdnHCl}]}{RT} \qquad (3)$$

where the kinetic $m^{\ddagger}$ value is usually interpreted as proportional to the solvent-accessible area that becomes exposed in the transition state. Fitting the kinetic data to this expression yields τ_0 and $m^{\ddagger}$ values of 17 ± 2 s and 0.74 ± 0.04 kcal mol^{-1} M^{-1}, respectively, for [C65S, C72S] and of 3.5 ± 0.3 s and 1.03 ± 0.02 kcal mol^{-1} M^{-1}, respectively, for [C40A, C95A].

DISCUSSION

Stability and Structure of [C40A,C95A] and [C65S, C72S] at 25 °C and pH 8.0. As noted in the Introduction, both the [C40A, C95A] and [C65S, C72S] mutants adopt nativelike conformations under folding conditions, based on their enzymatic activities (*18*), their NMR spectra (*19, 20*), and the X-ray structure of the [C40A, C95A] mutant (*16*). However, their equilibrium GdnHCl transitions indicate that the [C40A, C95A] mutant is significantly less stable than the [C65S, C72S] mutant, and both mutants are significantly less stable than wild-type RNase A (Table 1). The standard free-energy differences, $\Delta G°$, between the folded and unfolded states of the [C40A, C95A] and [C65S, C72S] mutants are 3.0 and 5.0 kcal/mol, respectively, compared with 11.3 kcal/mol for the wild-type protein (Table 1). The free-energy differences for the mutants are in qualitative agreement with thermal transition temperatures measured at pH 6.4 and 4.6 (*18*−*20*).

The difference in stabilities caused by the reduction of these two disulfides is unexpectedly large, and derives from

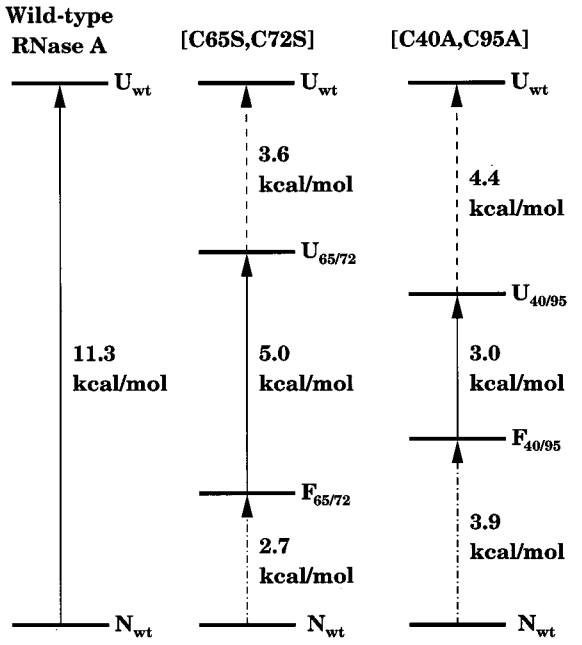

FIGURE 6: A free-energy diagram (at 25 °C and pH 8.0) for wild-type RNase A and the three-disulfide mutants [C65S, C72S] and [C40A, C95A]. The solid transition lines indicate the conformational stabilities of the three proteins, as measured by their GdnHCl transitions (Table 1). The dashed transition lines indicate the free-energy differences between the unfolded states of the three proteins, as estimated by the Wang-Uhlenbeck method (*39*). By subtracting these two contributions from the total conformational stability of the wild-type protein (11.3 kcal/mol), one can determine the free-energy difference between the native wild-type state N_{wt} and the folded states of the mutants, yielding 2.7 and 3.9 kcal/mol for the [C65S, C72S] and [C40A, C95A] mutants, respectively. The arrows indicate the direction of increasing standard free energy.

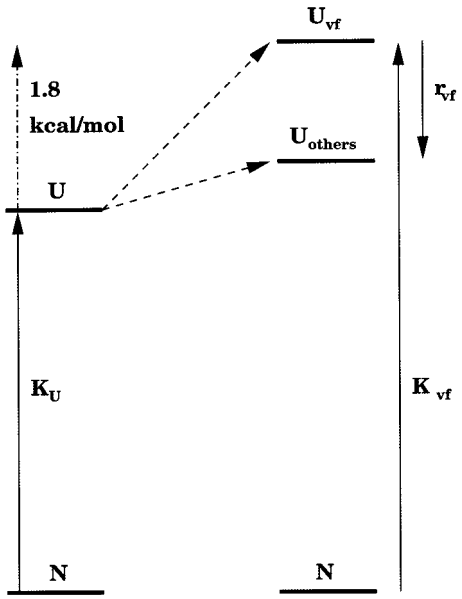

FIGURE 7: The unfolded species U_{vf} is 1.8 kcal/mol higher in free energy than the equilibrium unfolded species U (Appendix A). U_{vf} represents the conformationally unfolded species with all essential prolines in their native isomeric state, while U_{others} represents the conformationally unfolded species with at least one proline in a non-native isomeric state; together, U_{vf} and U_{others} comprise the equilibrium unfolded species U. This diagram also defines the ratios of concentrations K_U, K_{vf}, and r_{vf}, corresponding to the concentration ratios between U and N, U_{vf} and N, and U_{others} and U_{vf}, respectively, as indicated by the directions of the solid arrows. For RNase A, the ratio r_{vf} has been measured as 19 (95%/5%) (*10*).

a stabilization of the *unfolded* state as well as from a destabilization of the *folded* state. The change in the free energy of the unfolded state due to disulfide reduction can be estimated by the increase of its loop entropy computed by the Wang−Uhlenbeck method (*39*). However, the loop entropy at 25 °C accounts for only 3.6 and 4.4 kcal/mol of destabilization in the [C65S, C72S] and [C40A, C95A] mutants, respectively. The standard free energies of the *folded* states of the mutants relative to that of wild-type RNase A can be estimated by subtracting both the measured standard free-energy differences, $\Delta G°$, and the free-energy difference due to the loop entropy from the standard free energy of the *unfolded* state of wild-type RNase A (Figure 6). Thus, the folded conformations of [C65S, C72S] and [C40A, C95A] are less stable than the native wild-type protein by 2.7 and 3.9 kcal/mol, respectively, at 25 °C and pH 8.0. Recent NMR experiments have confirmed qualitatively that both folded mutants are less stable than the folded wild-type protein (*19*, *20*). These studies noted that reduction of each disulfide bond results in a strong *local* destabilization as well as a weaker *global* destabilization; hence, it is not possible to assign the destabilization free energy to a single conformational change.

The $\Delta G°$ values presented in Table 1 do not distinguish between the contributions from purely conformational unfolding and from the isomerization of prolines in the denatured state. Assuming that the prolines of the folded state are in the native isomeric state of the wild-type protein, the decrease in free energy due to the isomerization of all three essential prolines is roughly 1.8 kcal/mol (Appendix A). Thus, the purely conformational component of the standard free-energy difference, $\Delta G°_{vf}$, in the two mutants [C40A, C95A] and [C65S, C72S] is 4.8 and 6.8 kcal/mol, respectively, simply by adding 1.8 kcal/mol to the free-energy differences $\Delta G°$ reported in Table 1. The free-energy relationships are summarized in Figures 6 and 7.

Global versus Partial Unfolding in the Reduction of des-[40−95] and des[65−72]. The free-energy differences (4.8 and 6.8 kcal/mol, respectively) for *conformational* unfolding of these mutants are relevant for the reductive unfolding pathway of RNase A. In particular, the disulfide reduction reactions for the two structured intermediates, des[65−72] and des[40−95], have been modeled (*15*) by an EX2 reaction scheme (*40*) where the structured intermediate must first undergo some conformational unfolding to a state U* before reduction can occur

$$\text{des}[65-72] \rightleftharpoons U^*_{65-72} \xrightarrow{\text{DTT}^{red}} 2S + \text{DTT}^{ox} \qquad (4)$$

$$\text{des}[40-95] \rightleftharpoons U^*_{40-95} \xrightarrow{\text{DTT}^{red}} 2S + \text{DTT}^{ox} \qquad (5)$$

The free-energy difference between the folded state and the rate-limiting unfolded state U* of des[40−95] and des[65−72] has been estimated as 4.5 and 5.7 kcal/mol, respectively (*15*). Key questions are whether the rate-limiting unfolding step for these reduction reactions is global or local, and whether proline isomerization is involved.

A comparison of the free energies for the conformational and reductive unfolding reactions indicates that [C40A, C95A] most likely is reduced to 2S through global conformational unfolding, while the reduction of [C65S, C72S] involves partial unfolding and, possibly, the isomerization

of Pro93. As noted above, the free energy of purely conformational unfolding for [C40A, C95A] is roughly 4.8 kcal/mol while that of reductive unfolding is 4.5 kcal/mol (*15*). The close agreement of these two values makes it plausible that [C40A, C95A] unfolds globally before being reduced to the 2S species. Therefore, it is likely that all of the disulfide bonds of [C40A, C95A] will be susceptible to reduction in this reaction. By contrast, the free energy of purely conformational unfolding for [C65S, C72S] is 6.8 kcal/mol while that of reductive unfolding is 5.7 kcal/mol (*15*), suggesting that [C65S, C72S] is reduced to 2S through a *partial* unfolding step. Consequently, the 40−95 disulfide bond in des[65−72] may be preferentially reduced with respect to the other two disulfide bonds, under these conditions.

Possible Coupling of Proline Isomerization to Disulfide Reduction. The kinetic analysis of reductive unfolding (*15*) concluded that the reduction of the 40−95 and 65−72 disulfide bonds in wild-type RNase A and in des[65−72] is rate-limited by two *independent* unfolding reactions, in each of which the protein is unfolded in the vicinity of its corresponding disulfide bond without affecting the conformation at the other. One candidate for these reactions is the cis−trans isomerization of prolines near each disulfide, as discussed in the Introduction. Here it is shown that the free-energy change associated with the isomerization of Pro93 from cis to trans is consistent with the free-energy change associated with the reduction of the 40−95 disulfide bond.

The free-energy changes for these proline isomerizations can be estimated from previous work on site-directed mutants of the prolines (*9*, *41*). Comparison of the GdnHCl transitions of P93A and P114A to that of the wild-type protein indicates that non-native isomers of these prolines destabilize the folded *wild-type* protein by 5.3 and 1.9 kcal/mol, respectively (*9*) (Appendix A). The free-energy difference for Pro114 (1.9 kcal/mol) is much smaller than those observed (4.5−6.7 kcal/mol) in reductive unfolding (*15*); thus, the isomerization of Pro114 from cis to trans does not appear to play a significant role in reductive unfolding. By contrast, the destabilization caused by the isomerization of Pro93 from cis to trans (5.3 kcal/mol) is relatively close to that of the unfolding step for the reduction of des[65−72] (5.7 kcal/mol (*15*)), consistent with the hypothesis that the isomerization of Pro93 is the rate-limiting conformational change for the reduction of des-[65−72] to the 2S species. This model offers a plausible structural explanation of why the 40−95 disulfide bond is preferentially reduced in the des[65−72] intermediate (*15*). Moreover, if the isomerization of Pro93 is rate-limiting in the reduction of the native protein to the des[40−95] species as proposed, the newly formed des[40−95] species will initially have a non-native Pro93 isomer and thus be globally unfolded, judging from the conformational stability (3.0 kcal/mol) of its [C40A, C95A] analogue, which is much less than the destabilization caused by a non-native Pro93 isomer in the wild-type protein (5.3 kcal/mol). This kinetic mechanism may explain the extraordinarily rapid reduction of des[40−95] to the 2S species at 25 °C (*15*).

The kinetic experiments (*15*) and the proposed coupling of proline isomerization pertain to reductive unfolding under solution conditions favoring conformational folding, for example, neutral pH, low temperature, and low denaturant concentration. By contrast, under denaturing conditions, reductive unfolding is very likely *not* coupled to proline isomerization, since global unfolding has already occurred. Under such conditions, the disulfide bonds of the protein are not protected from the redox reagent and are reduced rapidly (*22*).

The Kinetics of Unfolding. Similar to the wild-type protein, the fluorescence-monitored unfolding of both mutants exhibits two exponential phases, a fast phase and a slow phase. It has been shown conclusively in wild-type RNase A that the slow phase corresponds to the isomerization of two prolines, Pro93 and Pro114 (*9*). Given that the amplitudes and time constants of the slow phase are similar to those of the wild-type protein and are independent of pH and GdnHCl concentration, it is reasonable to conclude that the slow phase of the mutants corresponds to the isomerizations of Pro93 and Pro114 as in wild-type RNase A and, moreover, that their cis/trans ratios in the folded and unfolded states are the same as that of wild-type RNase A. In particular, we conclude that Pro93 and Pro114 are both fully cis in the folded conformation of the mutants, consistent with the published NMR data (*19*, *20*) and the X-ray structure of [C40A, C95A] (*16*). The NMR and X-ray data also indicate that Pro117 is in its native trans isomeric state (*16*, *19*, *20*).

Therefore, both folded mutants have all of the essential prolines of RNase A (Pro93, Pro114, and Pro117) fully in their native isomeric state. This point is important to establish, since we propose that the reduction of the disulfides is rate-limited by the isomerization of prolines. This mechanism would be invalid if the prolines were in a non-native isomeric state in the folded mutants, or if isomeric heterogeneity were observed, as in some proteins (*42*).

Our results also suggest that the 40−95 disulfide bond is *not* responsible for the fluorescence quenching of Tyr92, contrary to an earlier proposal (*24*). On the basis of model peptide studies from our laboratory (*43*), it seems likely that short-range interactions are responsible for the fluorescence quenching of Tyr92 which is relieved by the cis-trans isomerization of Pro93, possibly between local peptide bonds and the tyrosine ring (*44*). However, the 40−95 disulfide bond may make a small contribution to the quenching, whose measurement would require more sensitive tests.

The fast conformational unfolding rate increases exponentially with the GdnHCl concentration and is characterized by the kinetic $m^{\ddagger}$ value. The ratio of this $m^{\ddagger}$ value to the equilibrium m value is relatively small, 0.19 and 0.26 for the [C65S, C72S] and [C40A, C95A] mutants, respectively. These small ratios indicate that the transition state for conformational unfolding exposes relatively little solvent-accessible area (*45*). This is consistent with wild-type RNase A, for which the ratio is 0.15 at pH 4.0 and 15 °C and 0.10 at pH 5.8 and 22 °C (*25*), indicating that the unfolding pathway is not altered dramatically by the reduction of the 40−95 or 65−72 disulfide bonds.

CONCLUSIONS

The equilibrium stability and conformational unfolding kinetics have been investigated for two RNase A mutants, [C40A, C95A] and [C65S, C72S]. The loss of each disulfide bond strongly destabilizes RNase A, even more than expected from the increase in loop entropy, in agreement with previous X-ray and NMR data (*16*, *19*, *20*). The conformational

stability, $\Delta G°$, of the [C40A, C95A] mutant indicates that the des[40−95] intermediate is reduced by global conformational unfolding, while that of the [C65S, C72S] mutant indicates that the des[65−72] intermediate is reduced by partial unfolding. This contrasts with studies on BPTI showing that reductive unfolding proceeds only through global unfolding (*46*). The values are consistent with the hypothesis that the reduction of the 40−95 disulfide bond in the folded forms of wild-type RNase A and of the des-[65−72] intermediate is rate-limited by the isomerization of Pro93 to its non-native trans isomer. This hypothesis is currently under investigation in our laboratory.

The conformational unfolding of both mutants exhibits two phases when monitored by fluorescence, similar to wild-type RNase A. The slow phase is almost certainly due to the isomerizations of Pro93 and Pro114, as in wild-type RNase A (*9*). The amplitudes of the slow phase indicate that Pro93 and Pro114 are both fully cis in both mutants, and that the 40−95 disulfide bond is *not* responsible for the fluorescence quenching of Tyr92 relieved by the isomerization of Pro93, contrary to an earlier proposal (*24*). A comparison of the kinetic $m^{‡}$ and equilibrium m values suggests that the unfolding pathway is not dramatically altered by the reduction of the 40−95 or 65−72 disulfide bonds, consistent with other proteins (*47*).

ACKNOWLEDGMENT

We thank D. Juminaga for experimental assistance and many helpful discussions. M. Iwaoka thanks the Yamada Science Foundation (Osaka, Japan) for a research fellowship during his stay at Cornell University.

APPENDIX A: THE FREE ENERGY OF SUB-SPECIES

The conformational stability of a protein is defined as the standard free-energy difference, $\Delta G°$, between its folded and unfolded states. However, the unfolded state of RNase A is not homogeneous; it is composed of eight species corresponding to the isomeric states of the three essential prolines (Pro93, Pro114, and Pro117) (*10*). The relative fraction of the protein in each of these unfolded species has been determined for one set of unfolding conditions (pH 2.0 at 15 °C) (*10*). These relative fractions depend on the relative rates of isomerization of the three essential prolines under unfolding conditions, which do not vary with pH and have the same activation energies (*9*); thus, these relative fractions are expected to apply to the solution conditions (pH 8.0 and 25 °C) used here.

This Appendix computes the free-energy difference between the folded species and a *subset*, even one, of the species that comprise the unfolded state. In particular, we seek to compute the free-energy difference between the native state N and the conformationally unfolded species U_{vf} which has all of its prolines in the native isomeric state. At equilibrium, U_{vf} constitutes 5.0% of the protein in the unfolded state U (*10*).

Consider Figure 7. Let K_U, K_{vf}, and r_{vf} represent, respectively, the ratios of equilibrium concentrations of the unfolded protein U to that of the native species N, of the conformationally unfolded species U_{vf} (with native prolines) to that of the native species N, and of the remaining unfolded species U_{others} (with at least one non-native proline) to that of the conformationally unfolded protein U_{vf}. Mathematically

$$K_U \equiv [U]/[N] \tag{A1}$$

$$K_{vf} \equiv [U_{vf}]/[N] \tag{A2}$$

$$r_{vf} \equiv [U_{others}]/[U_{vf}] \tag{A3}$$

These three quantities are related by the equation

$$\frac{[U]}{[N]} = \frac{[U_{vf}]}{[N]} + \frac{[U_{others}]}{[N]} \tag{A4}$$

$$K_U = K_{vf} + \frac{[U_{vf}][U_{others}]}{[N]\ \ [U_{vf}]} \tag{A5}$$

$$= K_{vf} + K_{vf}\, r_{vf} \tag{A6}$$

Therefore, the following relation holds

$$K_{vf} = \frac{K_U}{1 + r_{vf}} \tag{A7}$$

This relationship can be re-expressed in terms of free energies using the well-known relation between standard free-energy differences and the ratio K_{eq} of equilibrium concentrations, $\Delta G° = -RT \ln K_{eq}$. Taking the logarithms of both sides of equation A7, we obtain

$$\Delta G°_{fv} = \Delta G°_U + RT \ln(1 + r_{vf}) \tag{A8}$$

As noted above, U_{vf} constitutes 5% of the unfolded species U (*10*); thus, the ratio r_{vf} equals 19 (95%/5%), yielding a standard free-energy increase at 25 °C of 1.8 kcal/mol, as cited in the text. It should be noted that the standard free energy of a pure sub-species, for example, U_{vf}, is always higher than that of the equilibrium distribution, for example, U. In other words, the increase in $\Delta G°$ is always positive, regardless of the value of r_{vf}; allowing U_{vf} to equilibrate with the other proline isomeric states lowers the standard free energy, as expected from entropy considerations.

As another example, consider the free-energy difference between the native state N and the subset (denoted by U_{trans}) of four unfolded species with a trans isomer for a specific proline (Figure 8). Following the same argument as above, the concentration ratios may be defined

$$K_{wt} \equiv [U_{wt}]/[N_{wt}] \tag{A9}$$

$$K_{trans} \equiv [U_{trans}]/[N_{wt}] \tag{A10}$$

$$r_{trans} \equiv [U_{cis}]/[U_{trans}] \tag{A11}$$

where U_{cis} represents the complementary species to U_{trans}, that is, the subset of four species with the specified proline in the cis isomeric state. The following corresponding relation may be derived.

$$\Delta G°_{trans} = \Delta G°_{wt} + RT \ln(1 + r_{trans}) \tag{A12}$$

For Pro93, the ratio r_{trans} for the species U_{trans} is 1/3.4 (*10*), giving an increase in standard free energy of 0.15 kcal/mol

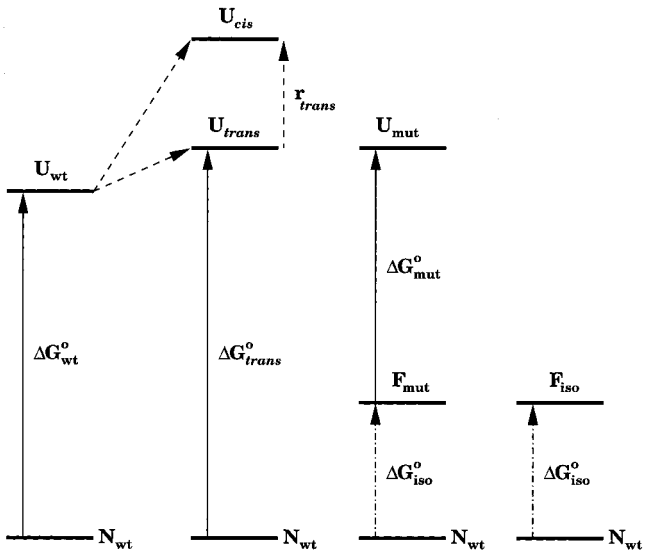

FIGURE 8: Illustration of how the conformational destabilization of a non-native proline isomer in the conformationally folded (but non-native) wild-type protein was estimated. First, a proline-to-alanine mutant such as P114A with its peptide group in the all-trans state is prepared and its conformational stability ΔG°_{mut} is measured (*9*). By assumption, the unfolded state U_{mut} of this mutant has a standard free energy equal to that of the unfolded state U_{trans} of the wild-type protein restricted to the trans isomer. The standard free energy ΔG°_{trans} can be estimated from the conformational stability ΔG°_{wt} of the wild-type protein and from the ratio r_{trans} of the fractions of the unfolded protein in the trans and cis isomeric states, as described in Appendix A. Subtracting ΔG°_{mut} from ΔG°_{trans} gives the free-energy difference ΔG°_{iso} between the folded state F_{mut} of the mutant protein and the native wild-type protein N_{wt}. By assumption, ΔG°_{iso} estimates the standard free-energy difference between the native state N_{wt} and the state F_{iso} of the wild-type protein, which is (by definition) conformationally folded with a non-native trans proline isomer, for example, the I_N folding intermediate (*10*).

over the full unfolded state U_{wt} at 15 °C. Alternatively, for the subset of unfolded species with a (non-native) trans Pro114, the ratio r_{trans} equals 1/2.6, giving an increase of 0.19 kcal/mol. These small corrections were added to the measured conformational stability ΔG°_{wt} of wild-type RNase A (*9*) to obtain ΔG°_{trans} for the subsets of unfolded species with Pro93 and Pro114 fixed in the non-native trans isomeric state. The conformational stabilities ΔG°_{mut} of the mutants (*9*) (6.1 and 9.6 kcal/mol for the P93A and P114A mutants, respectively) were subtracted from the computed ΔG°_{trans} (11.4 and 11.5 kcal/mol, respectively) to estimate the destabilization ΔG°_{iso} (5.3 and 1.9 kcal/mol, respectively) caused by non-native proline isomers in the conformationally folded (but non-native) *wild-type* protein (Figure 8). An example of such a state is the folding intermediate I_N, which is conformationally folded with nativelike enzymatic activity (*48*), but which has Pro93 in a non-native trans isomer (*10*).

REFERENCES

1. Levinthal, C. (1968) *J. Chim. Phys. 65*, 44−45.
2. Kim, P. S., and Baldwin, R. L. (1982) *Annu. Rev. Biochem. 51*, 459−489.
3. Kim, P. S., and Baldwin, R. L. (1990) *Annu. Rev. Biochem. 59*, 631−660.
4. Neira, J. L., and Rico, M. (1997) *Folding Des. 2*, R1−R11.
5. Cuchillo, C. M., Vilanova, M., and Nogués, M. V. (1997) in *Ribonucleases: Structures and Functions* (D'Alessio, G., and Riordan, J. F., Eds.) pp 271−304, Academic Press, San Diego, CA.
6. Raines, R. T. (1998) *Chem. Rev. 98*, 1045−1065.
7. Wlodawer, A., Svensson, L. A., Sjölin, L., and Gilliland, G. L. (1988) *Biochemistry 27*, 2705−2717.
8. Koradi, R., Billeter, M., and Wüthrich, K. (1996) *J. Mol. Graphics 14*, 51−55.
9. Juminaga, D., Wedemeyer, W. J., and Scheraga, H. A. (1998) *Biochemistry 37*, 11614−11620.
10. Juminaga, D., Wedemeyer, W. J., Garduño-Júarez, R., McDonald, M. A., and Scheraga, H. A. (1997) *Biochemistry 36*, 10131−10145.
11. Rothwarf, D. M., Li, Y.-J., and Scheraga, H. A. (1998) *Biochemistry 37*, 3760−3766.
12. Rothwarf, D. M., Li, Y.-J., and Scheraga, H. A. (1998) *Biochemistry 37*, 3767−3776.
13. Iwaoka, M., Juminaga, D., and Scheraga, H. A. (1998) *Biochemistry, 37*, 4490−4501.
14. Xu, X., and Scheraga, H. A. (1998) *Biochemistry 37*, 7561−7571.
15. Li, Y.-J., Rothwarf, D. M., and Scheraga, H. A. (1995) *Nat. Struct. Biol. 2*, 489−494.
16. Pearson, M. A., Karplus, P. A., Dodge, R. W., Laity, J. H., and Scheraga, H. A. (1998) *Protein Sci. 7*, 1255−1258.
17. Schultz, D. A., Friedman, A., and Fox, R. O. (1993) *Protein Sci. 2*, Suppl. 1, 67.
18. Laity, J. H., Shimotakahara, S., and Scheraga, H. A. (1993) *Proc. Natl. Acad. Sci. U.S.A. 90*, 615−619.
19. Laity, J. H., Lester, C. C., Shimotakahara, S., Zimmerman, D. E., Montelione, G. T., and Scheraga, H. A. (1997) *Biochemistry 36*, 12683−12699.
20. Shimotakahara, S., Rios, C. B., Laity, J. H., Zimmerman, D. E., Scheraga, H. A., and Montelione, G. T. (1997) *Biochemistry 36*, 6915−6929.
21. Talluri, S., Rothwarf, D. M., and Scheraga, H. A. (1994) *Biochemistry 33*, 10437−10449.
22. Iwaoka, M., and Scheraga, H. A. (1998) *J. Am. Chem. Soc. 120*, 5806−5807.
23. Pace, C. N. (1986) *Methods Enzymol. 131*, 266−280.
24. Rehage, A., and Schmid, F. X. (1982) *Biochemistry 21*, 1499−1505.
25. Houry, W. A., Rothwarf, D. M., and Scheraga, H. A. (1995) *Nat. Struct. Biol. 2*, 495−503.
26. Rothwarf, D. M., and Scheraga, H. A. (1993) *Biochemistry 32*, 2671−2679.
27. Denton, J. B., Konishi, Y., and Scheraga, H. A. (1982) *Biochemistry 21*, 5155−5163.
28. Thannhauser, T. W., Konishi, Y., and Scheraga, H. A. (1987) *Methods Enzymol. 143*, 115−119.
29. Nozaki, Y. (1972) *Methods Enzymol. 26*, 43−50.
30. Santoro, M. M., and Bolen, D. W. (1988) *Biochemistry 27*, 8063−8068.
31. Houry, W. A., Rothwarf, D. M., and Scheraga, H. A. (1994) *Biochemistry 33*, 2516−2530.
32. Marquardt, D. W. (1963) *J. Soc. Ind. Appl. Math. 11*, 431−441.
33. Scheraga, H. A. (1967) *Fed. Proc. 26*, 1380−1387.
34. Grathwohl, C., and Wüthrich, K. (1981) *Biopolymers 20*, 2623−2633.
35. Sendak, R. A., Rothwarf, D. M., Wedemeyer, W. J., Houry, W. A., and Scheraga, H. A. (1996) *Biochemistry 35*, 12978−12992.
36. Hermans, J., Jr., and Scheraga, H. A. (1961) *J. Am. Chem. Soc. 83*, 3283−3300.
37. Pace, C. N., Laurents, D. V., and Thomson, J. A. (1990) *Biochemistry 29*, 2564−2572.
38. Burgess, A. W., and Scheraga, H. A. (1975) *J. Theor. Biol. 53*, 403−420.
39. Lin, S. H., Konishi, Y., Denton, M. E., and Scheraga, H. A. (1984) *Biochemistry 23*, 5504−5512.
40. Woodward, C., Simon, I., and Tüchsen, E. (1982) *Mol. Cell. Biochem. 48*, 135−160.

41. Dodge, R. W., and Scheraga, H. A. (1996) *Biochemistry 35*, 1548−1559.
42. Raleigh, D. P., Evans, P. A., Pitkeathly, M., and Dobson, C. M. (1992) *J. Mol. Biol. 228*, 338−342.
43. Haas, E., Montelione, G. T., McWherter, C. A., and Scheraga, H. A. (1987) *Biochemistry 26*, 1672−1683.
44. Cowgill, R. W. (1976) Tyrosyl Fluorescence in Proteins and Model Peptides, in *Biochemical Fluorescence: Concepts*, Vol. 2, pp 441−486.
45. Tanford, C. (1970) *Adv. Protein Chem. 24*, 1−95.
46. Ma, L.-C., and Anderson, S. (1997) *Biochemistry 36*, 3728−3736.
47. Vanhove, M., Guillaume, G., Ledent, P., Richards, J. H., Pain, R. H., and Frére, J.-M. (1997) *Biochem. J. 321*, 413−417.
48. Schmid, F. X., and Blaschek, H. (1981) *Eur. J. Biochem. 114*, 111−117.

BI982593K